

Ballistic Impact Fracture Behaviour of Continuous Fibre Reinforced Al-Matrix Composites.

Al-Hamdan Ali^{*}, Yassin L. Nimir, Ramadan J. Mustafa

Faculty of Engineering, Mechanical Engineering Department, Mu'tah University, Jordan.

Abstract

The materials response under high energy impact loads was studied using a gas gun. The projectiles were pins 1.2-1.5 mm in diameter and weighing 0.347-0.435 g. The projectile velocity was in the range 100–1300 m/s. The remnant load carrying capability of composite samples after high velocity impact tests was measured to quantify high energy impact induced microstructural damage. The composites retained some of their load bearing capacity even after penetration of the projectile, since structural damage caused by projectiles remained localised, preventing catastrophic failure, particularly for continuous fibre reinforced Al_{pure} matrix composites. Penetration by the projectile occurred at impact energy of about 62-65 J for the conditions investigated. The experimental findings show that the energy absorbing capacity of such composites and their ability to withstand a given blow are largely functions of fibre type and greatly influenced by the matrix ductility, fibre-matrix interfacial bonding and volume fraction of reinforcing fibre. Understanding crack propagation and damage development under high energy impact loads may open new opportunities for the use of these composites in lightweight armour applications.

© 2010 Jordan Journal of Mechanical and Industrial Engineering. All rights reserved

Keywords: Fracture Behaviour, Composite materials, Fibre reinforced, Ceramic matrix, Metal matrix, High energy impact, High velocity.

1. Introduction

Since the 1960's, considerable interest has been given to metal-ceramic laminated composites armours because of their unique combination of strength, fracture toughness, high hardness and low density that make them ideal candidates for light weight protective systems [1-19]. At present they are developed to replace conventional matrix alloys and ceramic materials in specifically required engineering components. Very little work has been done on examining the impact response of ceramic fibre reinforced metal matrix composites at impact velocities above 500 m/s. Cantwell and Morton [5] have shown that the response of a Carbon fibre reinforced composites to low and high velocity impact loading was quite different. On the one hand, for low velocity impact, the size and shape of the panel determined its energy absorbing capability. Whereas, the high velocity projectiles induced a localised response in the target that did not depend on the

real size of the target. Cantwell et al. [21] have previously shown that below an impact energy of 50 J, the energy absorbed by 3 mm and 6 mm plates dropped off and appeared to approach an asymptotic level. For a 6- mm thick CFRP composite panel, the level of damage also appeared to drop off and approached a constant level whereas with the 3 mm target the level of damage appeared to be constant regardless of the impact energy. The observed constant level of damage in the 3 mm panel was probably due to the fact that the level of damage had already plateaued before the minimum impact velocity used in these experimental trials was reached. Indeed, Lee and sun [20] have shown that the drop off in a real damage occurred at an impact energy of 20 J for 4 and 5-mm diameter spheres impacting a 2-mm thick graphite/epoxy laminates. This was at much lower impact energy than was tested in [5]. Recent studies [3, 12, 18] on impact response of a variety of carbon-fibre-based laminates at velocities between 150 and 1000 m/s. In their work, they employed embedded PVDF stress gauges and constantan strain gauges to assess the stress and strain response of the

* Corresponding author: Hayajneh@mutah.edu.jo

materials when subjected to impact and penetration. They found that the maximum stress generated in the CFRPs depended on the nature of the reinforcing fibres. Further, they noted that above a critical measured stress, the fracture of the CFRP was “fluid-like” in that comminution of the material had occurred. They also observed, what they described as a “fluid-like” failure of the laminate. Notably, they showed that there was no clear difference in the energy absorbing abilities between cross-ply specimens and specimens consisting of a five-harness woven cloth. They also showed that the delamination width depended on impact energy. Here they showed that the maximum damage inflicted by the projectile at the ballistic limit was produced at normal incidence [3]. Furthermore, below the ballistic limit, the extent of damage for normal impact was larger than that for the oblique impact. However, the extent of damage at higher velocities appeared to be greater for oblique impacts. The objective of this study was to experimentally examine the response of a range of performs of continuous Silicon Carbide (SiC), high strength (HS) Carbon, and tungsten fibre reinforced Al_{pure} and Al-Si-Mg metal matrix materials under high energy impact loads using a gas gun. The remnant load carrying capability of composite samples after the high velocity impact tests was measured to quantify the high energy impact induced failure.

2. Experimental methodology

2.1. Materials

The composite materials utilized in this study were made from unidirectionally infiltrated 99.95% commercially pure aluminium Al_{pure} and aluminium alloy(6061) Alalloy matrix into performs of continuous high strength carbon (H.S.C), tungsten (w), and Silicon Carbide (SiC) fibres, and the mechanical properties of the constituents are shown in table 1-3. The composite material was manufactured by a liquid infiltration technique, Detailed information of the constituents and processing conditions can be found in [10-12]. Fibre volume fractions of unidirectional specimens were determined by optical numeric volume fraction analysis (ONVF) technique which is described in details in [13], and the analysis indicated that the volume fraction of fibres was consistent from plate to plate, with a volume fraction of 45%±3% for all composites.

The type and geometry of the test specimens were dictated by the size and quantity of the fabricated materials plates produced. Using a diamond saw, specimens with dimensions 75 x 10 x 3 mm were then cut from unidirectional material plates.

Table (1): Properties of the selected continuous fibre reinforcement, [9,2014,21]

Properties	High Strength Carbon fibre(H.S.C)	Silicon Carbide fibre (SiC)	Tungsten (w)
Fibre Diameter, μm	7-30	12-20	10-150
Density, Mg/m^3	1.75-1.9	2.5	19.2
Young's Modulus, GPa	230-270	190-200	400
Poisson's Ratio (ν)	0.2	0.25	-
Tensile Strength, GPa	3-4.8	2.5	2.5
Failure Strain, %	1.1	-	-
Thermal Expansivity, 10^{-6}K^{-1}	(-0.4)-(-1.2)	4.5	5
Thermal Conductivity, $\text{Wm}^{-1} \text{K}^{-1}$	24	-	-

Table (2): Chemical composition of Al (1100) and Al (6061) matrix materials by weight percentage, [8].

Alloy	Si	Mg	Cu	Ti	Fe	Mn	V	Cr	Zn	Be	Other elements
Al(1100)	0.25	0.05	0.05	---	0.04	0.05	0.05	---	---	---	0.03
Al(6061)	0.76	0.92	0.22	0.1	0.28	0.04	0.01	0.07	0.06	0.003	0.45

Table (3): Mechanical properties of Al (1100) and Al (6061) matrix materials, [8].

Material	E (GPa)	σ_{tensile} (MPa)	σ_{yield} (MPa)	Strain to failure (%)	Poisson ratio (ν)
Al(1100)	69	90	34	50-70	0.33
Al(6061)	72	310	275	12	0.33

2.2. High energy impact test and evaluation

High energy impact tests were carried out by impacting composite specimens of dimensions 75 mm 10 mm 3 mm with projectiles of varying velocities using a laboratory gas gun. The diameters of the 2024Al projectiles are in the range 1.22–1.28 mm, and weighing 0.347–0.435g. The projectile velocity range during this investigation was 100–1350 m/s with normal angle. The samples were mechanically clamped to a steel sample holder without a backing plate. The gun employed for this study was a single stage laboratory gas gun capable of firing spherical or cylindrical projectiles with diameters up to 1–12 mm at velocities up to 2500 m/s. A detailed description of the facility used is given by McQuillan [7] and a schematic diagram of the gas gun is shown in Figure 1. The gun uses compressed nitrogen gas to fire the projectile and is operated by a bursting-diaphragm firing mechanism. The compressed gas is transferred from the cylinder to the gas reservoir (on one end of the barrel), which is joined to a breech adaptor. A suitable diaphragm is placed between the barrel and the breech adaptor. The pressure in the reservoir causes the diaphragm to rupture, shooting the projectile through the barrel. The velocity of the projectile is controlled by the pressure, which is required to burst the diaphragm.

The macroscopic damage of the samples after impacts was recorded using a digital camera (Olympus D-510). At least five samples for each testing condition were considered; with the impression left by the high velocity

impact was placed in the centre of the sample. As-received and impacted samples were tested on a universal testing machine using a 4-point flexure fixture with 30-mm inner and 60-mm outer spans. Each specimen was placed in the fixture such that its impacted side was under tension and the point of impact was located in the centre of the inner spans. Tests were conducted at a speed of 1 mm/min using a 50 kN load cell. On the basis of data obtained during the 4-point bending tests, Young's modulus was calculated using the following relation:

$$E = \frac{Fl_0^2 l_1}{16Jy_0} \quad (1)$$

where,

$$J = \frac{bh^3}{12} \quad (2)$$

with: b , width of sample; h , height of sample; $l_1 = 15$ mm; $l_0 = 30$ mm; F , maximum load and y_0 , deflection at load F , measured using transducers. From the load–deflection curves the load for fracture initiation was recorded. A digital camera (Olympus D-510) was used to document the macroscopic deformation of the sample during 4-point flexure strength test. Fracture surfaces of selected samples were observed by scanning electron microscopy (SEM).

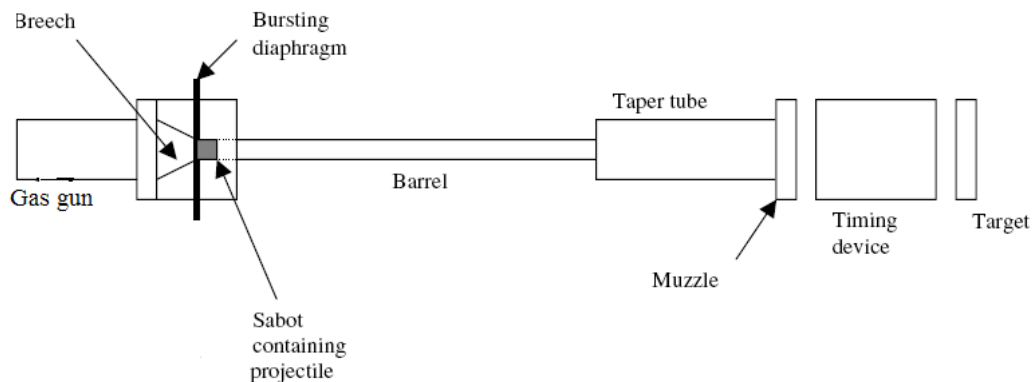


Figure 1 Schematic diagram of the testing apparatus used for the high energy impact tests.

3. Results and Discussion

3.1. High velocity impact resistance and damage

Low energy impacts are associated with delamination damage in fibre reinforced composite materials, and this inter-laminar debonding primarily may reduce the local bending stiffness and thus can affect the bending and buckling behaviour of the structure, by inducing further delamination growth which can lead to overall global weakening of the structure. Such damage has been

reported [15–21] to cause as much as a 40% reduction in static and fatigue strength. The results obtained for continuous fibre reinforced Al_{pure} and Al_{6061} matrix composites, when subjected to low energy projectile impacts, demonstrated a typical composite behaviour with the samples remaining in one piece despite some localised damage, Figure 2(a) shows the macroscopic damage caused by a projectile having impact energy of 17.25 J wherein a considerable number of fibres fracture, pulling-out on the front face of the sample can be seen.

Owing to the relatively low impact energy, the sample was not penetrated during this impact.

As impact energy increases, debonding coupled with fibre fragmentation, as in Figure 2(b) for a sample impacted with a projectile of 75.25 J energy, has occurred, with penetration of the projectile through the samples. This and Traces of force versus time of six impact events with incremental incident energies for W-Al_{pure} composite material, and force versus time histories and damage progression for unidirectional C-Al_{pure} shown in figures 3 and 4, respectively,. The samples for continuous fibre reinforced Al_{pure} stayed in one piece and with less damage compared to that of fibre reinforced Al₆₀₆₁, as in Figure 5, this is possibly due to the presence

of ductile matrix and a low fibre-matrix interfacial strength, giving rise to energy absorption mechanisms during high energy impact loads. However, due to the complex nature of the metal matrix composite microstructure, post-impact microscopic examination of the impacted surface did not reveal much structural detail. High energy impact [19-29] is defined by the energy required for a projectile to penetrate the rear face of the composite plate, however, from the results obtained for high energy impact seemed that the structural damage was highly localised around the point of impact, and the localised delamination and damage below the surface were easily detected by ultrasonic C-scan, as shown in Figure 6.

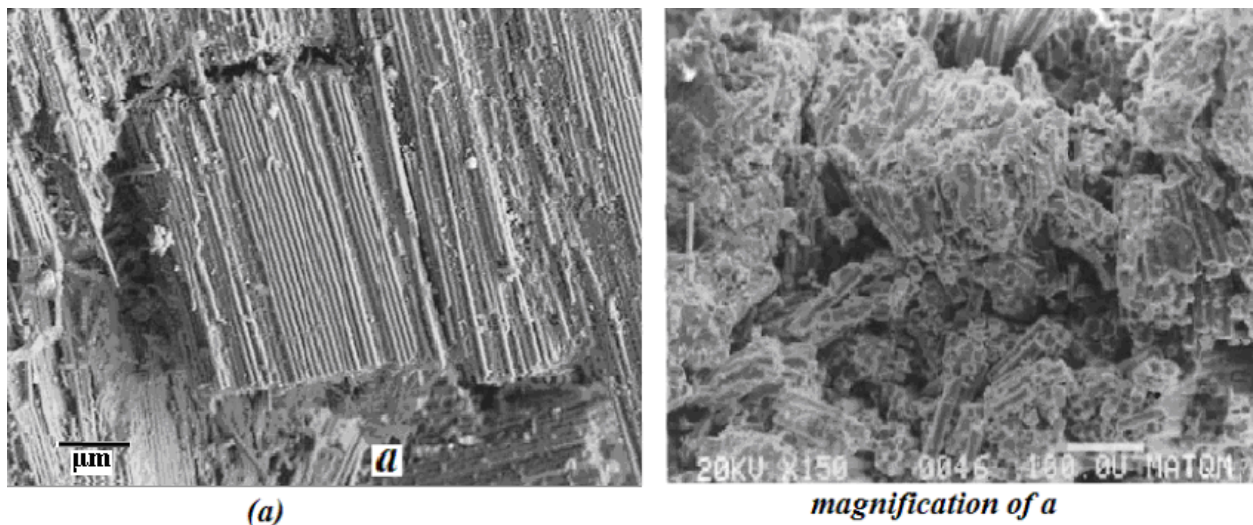


Figure 2(a) Micrographs showing the macroscopic damage of SiC-Al_{pure} matrix composite after high velocity impact test at impact energy of 17.25J

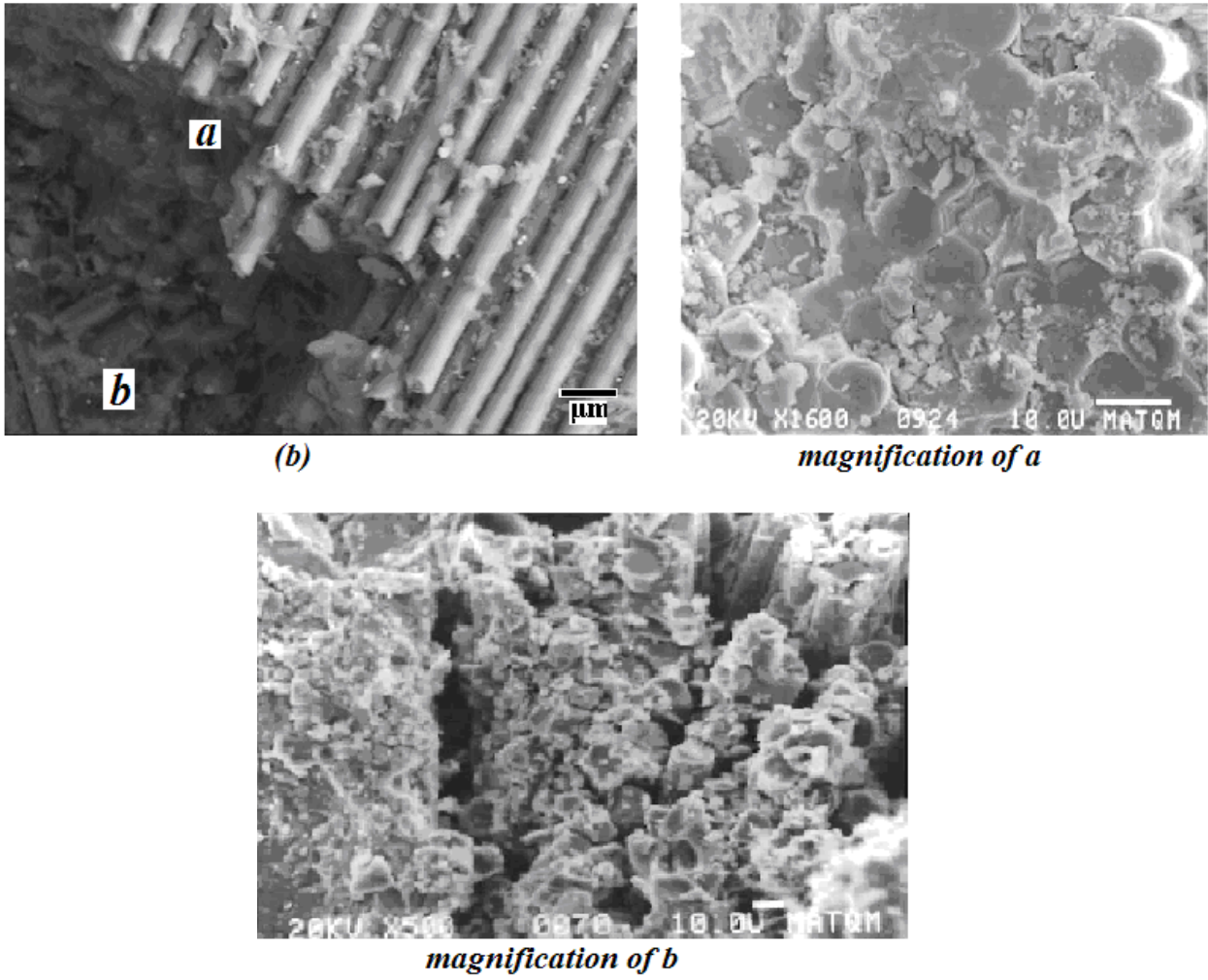


Figure 2(b) Micrographs of high energy impacted area (75.25J), showing debonding coupled with fibre fragmentation of C-Al_{pure} composite material, and the higher magnification of area a and b.

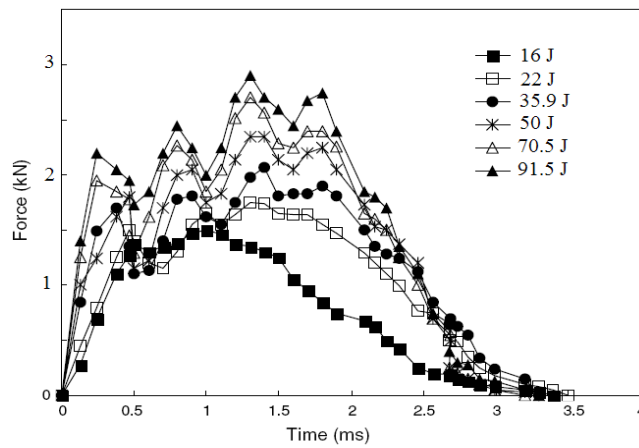


Figure 3(a) Force versus time traces of six impact events with incremental incident energies for w-Al_{pure} composite material.

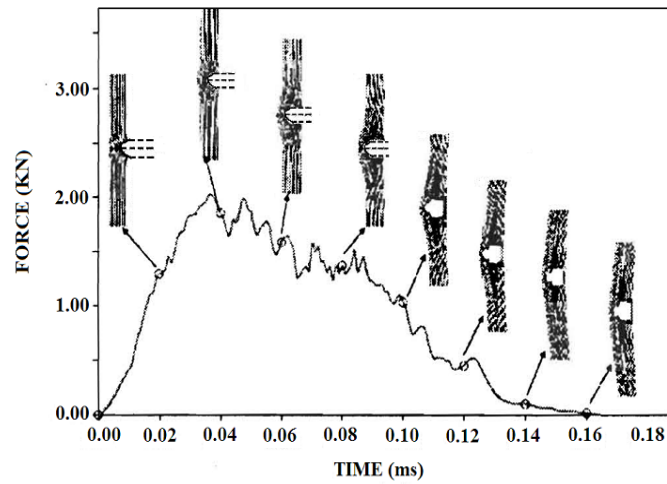


Figure 3(b) Force versus time histories and damage progression for w-Al_{pure} composite material, at an impact velocity of 670 m/s by 2024Al projectile.

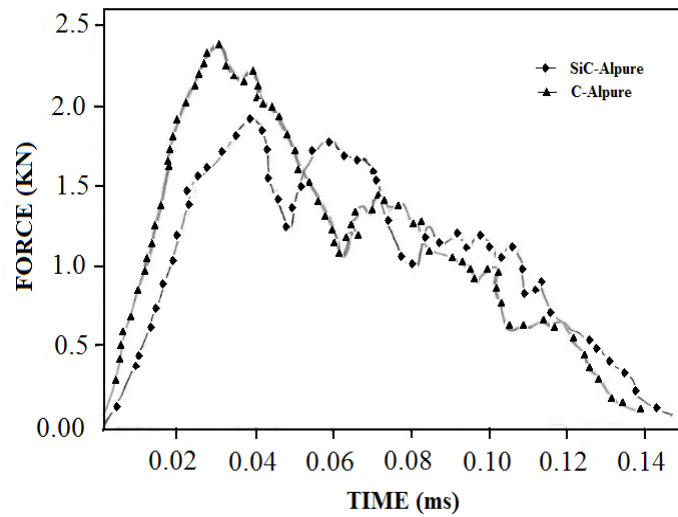


Figure 4 Force versus time histories for C-Al_{pure} and SiC-Al_{pure} composite material, at an impact velocity of 700 m/s by 2024Al projectile.

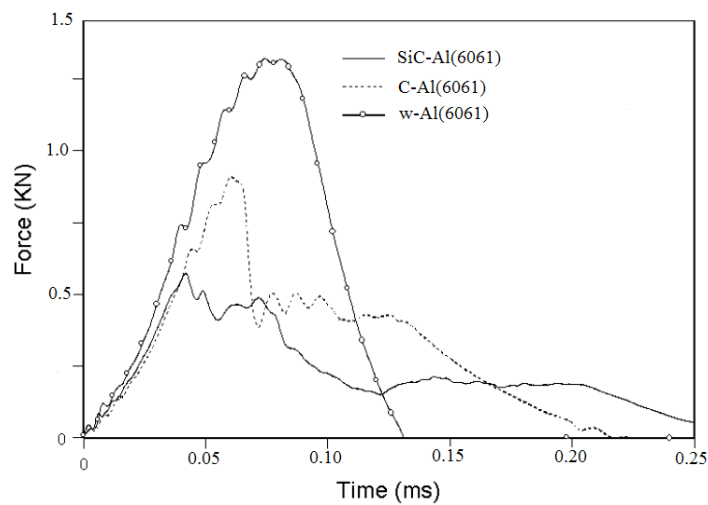


Figure 5 Force versus time histories for C-Al₆₀₆₁, SiC-Al₆₀₆₁, and w-Al₆₀₆₁ composite material, at an impact velocity of 700 m/s by 2024Al projectile.

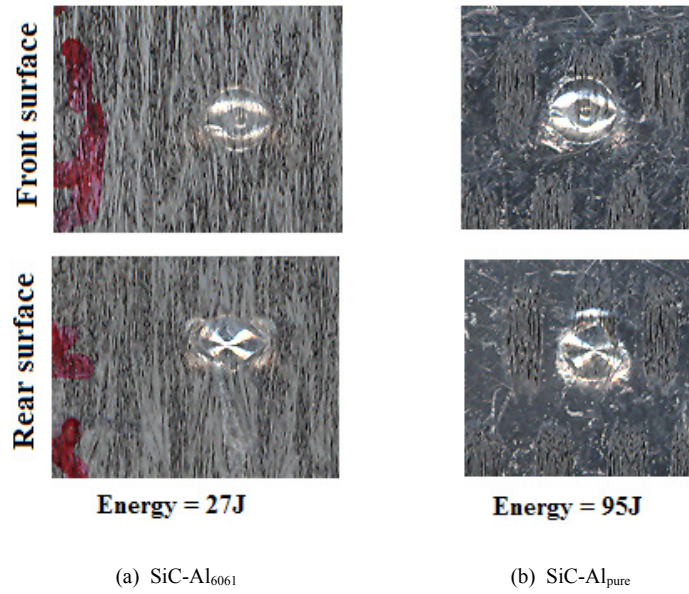


Figure 6(a) Insitu observations on the front and rear surface of specimens SiC-Al₆₀₆₁ and SiC-Al_{pure} composite materials.

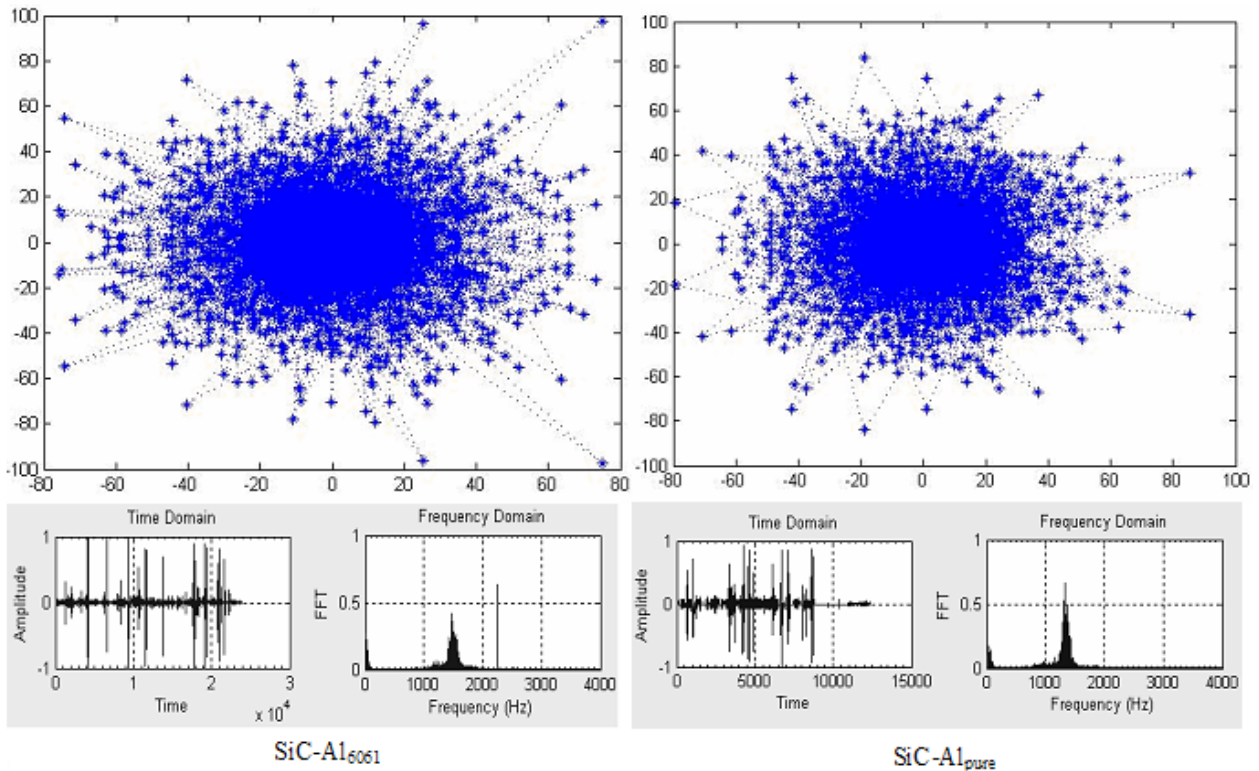


Figure 6 (b) C-scan plot of figure 6 (a) of impact sites on SiC-Al₆₀₆₁ and SiC-Al_{pure} composite material, impacted at 173.5 J, showing distinct craters concentration sites.

In order to assess the effects of high velocity impact energy on microstructural damage and on structural integrity of the composite, the damaged samples were subjected to 4-point flexural strength test. Fig.7 shows load–displacement curves for as-received (a), and impact damaged samples(b), (impact energy 85.01 J). with the impression left by the high velocity impact was in the

centre of the sample. As expected, the composite under investigation does not fail catastrophically, even after having been substantially damaged by the impact of projectiles. Instead, the material retains its load bearing capacity after the commencement of failure (penetration of the projectile). This behaviour is in agreement with literature reports [3,5,28] on continuous fibre reinforced

glass-epoxy matrix composites. Fig. 8 documents the high level of deformation achieved during 4-point flexural strength test in a sample of SiC- Al_{pure} , that had been

impacted at an energy of 27.76 J. The sample did not break into two fragments, demonstrating a true composite, "pseudo-plastic" behaviour.

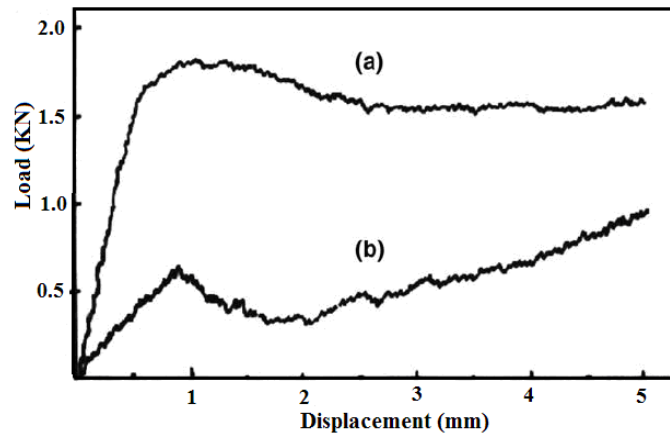


Figure 7 Load-displacement curves for: (a) as received and (b) impact damaged samples in 4-point flexural test for SiC- Al_{6061} composite material impacted at 85.01 J.

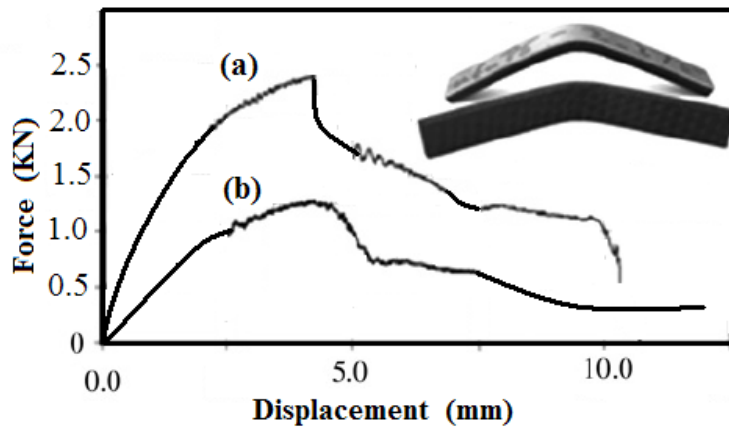
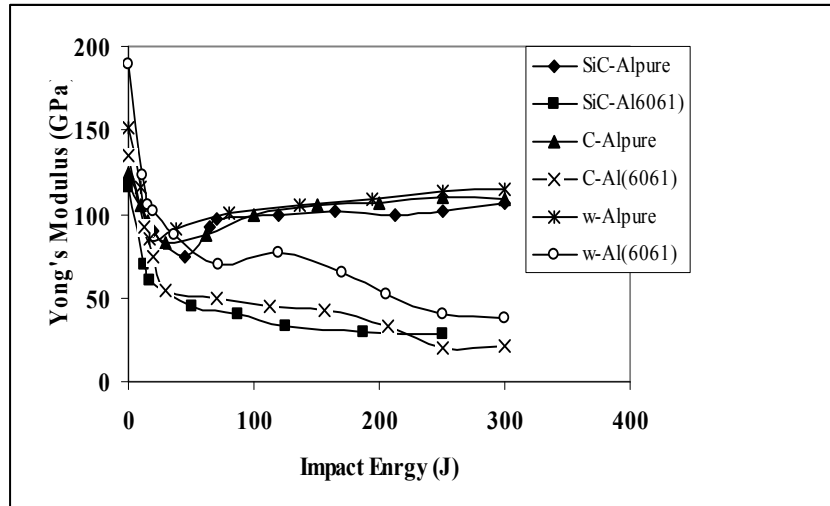


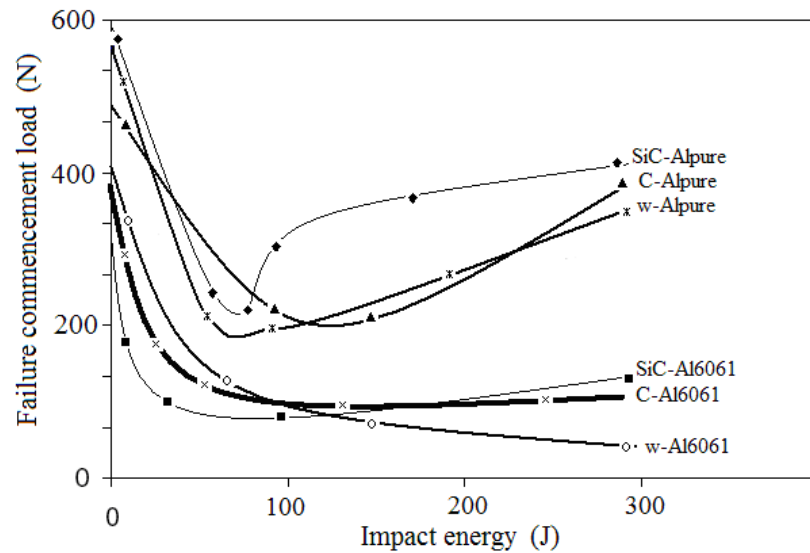
Figure 8 Load-displacement curves for: (a) as received and (b) impact damaged samples in 4-point flexural test for of SiC- Al_{pure} composite material impacted at 27.76 J. showing "pseudo-plastic" behaviour.

A plot of relative Young's modulus as a function of impact energy is presented in Fig.9 (a and b). A decrease in elastic modulus after high energy impact for all fibre reinforced Al_{pure} composite materials were observed up to the point of (62-65 J impact energy), whereas, the fibre reinforced Al_{6061} composite materials were observed up to the point of (15.6-27.76 J impact energy) where structural damage is maximum. Samples impacted with higher

energy projectiles show an increase in Young's modulus, particularly for fibre reinforced Al_{pure} matrix composites, indicating less structural damage. This is in accordance with the existing understanding that structural damage under high velocity impact increases to a point where impact energy is just sufficient to cause penetration as observed, in polymer and glass-ceramic matrix composites [28,29].



(a)



(b)

Figure 9(a) Elastic modulus and (b) fracture load of high velocity impacted Continuous fibre reinforced A_{pure} and Al_{6061} matrix composites as a function of impact energy. The values shown are averages of five measurements and the relative error was in all cases <10%.

The observed continuous decrease of Young's modulus with increasing impact energy of projectile (below 15.5 J), as in Fig.9 (a and b), which is related to the cumulative development of microstructural damage in the sample, may be analysed by considering a model linking elastic constants, macrocracking density, and matrix ductility. Assuming that macrocracking in the matrix is the dominant damage mechanism, the approach proposed by Silva MAG and S Ryan [24,26] for the elastic modulus of a cracked body could be appropriate, which introduces a damage parameter based on area and perimeter of uniformly distributed cracks. However the damage introduced in the present composites under increasing impact energy may involve more complex mechanisms than purely matrix micro or macrocracking, including matrix ductility, fibre-matrix interfacial debonding, localised multifracture of fibres, and fibre pullout. Thus a

predictive model for the high energy impact behaviour of the present composites must take into consideration the complex microstructure of the composites and the effect of matrix ductility and interfaces. The formulation of such a model is beyond the scope of the present experimental study. Considering the failure commencement load as an indicator of residual strength of the composite, it was found that this reaches a minimum value when the impact energy is just below that required for penetration of the projectile (Fig. 9(b)). Further increase in high impact energy after penetration of the sample by the projectile results in increase of the load carrying capability of the composite, due to less microstructural damage being introduced in the sample. This behaviour is in general agreement with the literature on high velocity impact resistance of composite materials [23,28,29].

4. Conclusion

Ceramic fibre reinforced Al_{pure} and Al₆₀₆₁ metal matrix composites, when subjected to high velocity impact loading by firing metallic cylindrical projectiles, retain some of their load bearing capacity after penetration by the projectile. This is due to the fact that structural damage caused by projectiles remains localised preventing catastrophic failure. For the conditions of the present tests, penetration by the projectile occurs at impact energy of about 17.5-27.5 J and 62-65 J for fibre reinforced Al₆₀₆₁ and Al_{pure} metal matrix composites, respectively, which indicates that there is a limiting value for the material to be useful in high energy impact armour applications when it is used on its own (without backing layers).

References

- [1] Børvik T, Langseth M, Hopperstad OS, Malo KA. Perforation of 12 mm thick steel plates by 20 mm diameter projectiles with flat, hemispherical and conical noses Part I: experimental study. *Int J Impact Eng* 2002;27:19–35A study of fragmentation in the ballistic impact of ceramics. *Int J Impact Eng* 1994;15:605–18.
- [2] Roy T, Chakraborty D. Delamination in hybrid FRP laminates under low velocity impact. *J Reinf Plast Compos*, Vol. 25, No. 18, 2006; 1939–56.
- [3] Lopez-Puente J, Zaera R, Navarro C. Experimental and numerical analysis of normal and oblique ballistic impacts on thin carbon/epoxy woven laminates. *Compos Part A Appl Sci*, Vol. 39, 2008, 374–87.
- [4] Millett JCF, Bourne NK, Meziere YJE, Vignjevic R, Lukyanov A. The effect of orientation on the shock response of a carbon fibre-epoxy composite. *Compos Sci Technol*, Vol. 67, 2007, 3253–60.
- [5] Cantwell WJ, Morton J. Comparison of the low and high velocity impact response of CFRP. *Composites*, Vol. 20, No. 6, 1989, 545–51.
- [6] Silvestrov VV, Plastinin AV, Gorshkov NN. Hypervelocity impact on laminate composite panels. *Int J Impact Eng*, Vol. 17, 1995, 751–62.
- [7] McQuillan F. PhD Thesis, Imperial College, University of London; 1992.
- [8] American Society for Metals, "Properties and Selection: Nonferrous alloy and pure metals", *Metals Handbook*, 9th edition, Vol.2, 1979, 63 and 161.
- [9] Ming Yang, V.D. Scott and R.L.Trumper, "The role of interface on the mechanical behaviour of carbon fibre reinforced aluminium alloy composites". *Metal Matrix Composites*, 2nd Conference, the Royal Society, U.K, 1989.
- [10] F.M.Hosking, F.Folgar-Portillo, R.Wunderlin, And R.Mehrabian, in "Composite of Aluminium alloys; Fabrication and Wear Behaviour", *J. Mat. Sci.*, 17, 1982, 477-98.
- [11] R. L. Trumper, P. J. Sherwood and A.W. Cifford, in "Metal Matrix Composites", *Proc. 1st Conf. on 'Materials in Aerospace*, 2-4 April, 1985, The Institute of Metals, London, 20.1-20.15.
- [12] R. L. Trumper, and V. D. Scott, in "Cast microstructures in fibre reinforced metals", 7th International Conference on the materials revolution through the 90's, paper 27, 1989.
- [13] M. C. Waterbury and L. T. Drzal, in "Determination of fibre volume fraction by optical numeric volume fraction analysis", *J. Reinforced Plastics and Composites*, Vol. 8, 1989, 627-636
- [14] Schonberg WP. *Key Engineering Materials* 1998;141–143:573–84.
- [15] George PE, Dursch HW. NASA Technical Reports Accession ID: 94N31036, Document ID: 19940026531; 1993.
- [16] Tennyson RC, Lamontagne C. Hypervelocity impact damage to composites. *Composites Part A*, Vol. 31, 2000, 785–94.
- [17] Übeyli M, Yıldırım RO, Ögel B. Investigation on the ballistic behavior of Al₂O₃/Al₂O₂₄ laminated composites. *J Mater Process Technol* Vol. 196, 2008, 356–64.
- [18] Übeyli M, Yıldırım RO, Ögel B. On the comparison of the ballistic performance of steel and laminated composite armours. *Mater Design* 2007;28(4):1257–62.
- [19] Wang B, Chou SM. The behavior of laminated composite plates as armour. *J Mater Process Technol*, Vol. 68, 1997, 279–87.
- [20] Lee S-WR, Sun CT. Dynamic penetration of graphite/epoxy laminates impacted by a blunt-ended projectile. *Compos Sci Technol*, Vol. 49, 1993, 369–80.
- [21] Cantwell WJ, Morton J. Impact perforation of carbon fibre reinforced plastics. *Compos Sci Technol* 1990;38:119–41
- [22] Woodward RL, Gooch Jr WA, O'Donnell RG, Perciballi WJ, Baxter BJ, Pattie SD. A study of fragmentation in the ballistic impact of ceramics. *Int J Impact Eng*, Vol. 15, 1994, 605–18.
- [23] Naik NK, Shirirao P, Reddy BCK. Ballistic behaviour of woven fabric composites: formulation. *Int J Impact Eng*, Vol. 32, No. 9, 2006, 1521–2.
- [24] Silva MAG, Cismas-iu C, Chiorean CG. Numerical simulation of ballistic impact on composite laminates. *Int J Impact Eng*, Vol. 31, No. 3, 2005, 289–306.
- [25] Berthelot JM, Sefrani Y. Longitudinal and transverse damping of unidirectional fibre composites. *Compos Struct*, Vol. 79, 2007, 423–31.
- [26] Ryan S, Schaefer F, Riedel W. Numerical simulation of hypervelocity impact on CFRP/Al HC SP spacecraft structures causing penetration and fragment ejection. *Int J Impact Eng*, Vol. 33, 2006, 703–12.
- [27] Tanabe Y, Aoki M, Fujii K, Kasano H, Yasuda E. Fracture behavior of CFRPs impacted by relatively high-velocity steel sphere. *Int J Impact Eng*, Vol. 28, 2003, 627–42.
- [28] Fujii K, Aoki M, Kiuchi N, Yasuda E, Tanabe Y. Impact perforation of CFRPs using high-velocity steel sphere. *Int J Impact Eng*, Vol. 27, 2002, 497–508.
- [29] Strassburger E, Lexow B, Ashuach H, Yeshurun Y, Bar-Ziv S, Hachamo Y, Gedon H. Impact on ceramic-metal-composites-ballistic resistance and fracture behavior *Proceedings of the 20th Symposium on Ballistics*, Orlando, FL, USA, 2002. 8pp.